



## Nonlocal Effect on Buckling of Triangular Nano-composite Plates

A. R. Shahidi<sup>a</sup>, A. Anjomshoa<sup>a</sup>, S. H. Shahidi<sup>a</sup>, E. Raeisi Estabragh<sup>\*b</sup>

<sup>a</sup> Department of Mechanical Engineering, Isfahan University of Technology, Isfahan, Iran

<sup>b</sup> Department of Mechanical Engineering, University of Jiroft, Jiroft, Iran

### PAPER INFO

#### Paper history:

Received 08 December 2015

Received in revised form 12 January 2016

Accepted 03 March 2016

#### Keywords:

Buckling Analysis

Small Scale Effect

Nonlocal Elasticity Theory

Triangular Nano-composite Plate

Galerkin Method

### ABSTRACT

In the present study, small scale effect on critical buckling loads of triangular nano-composite plates under uniform in-plane compression is studied. Since at nano-scale the structure of the plate is discrete and the long-range cohesive forces become important, the size dependent nonlocal elasticity theory is employed to develop an equivalent continuum plate model for this nanostructure incorporating the change in its mechanical behavior. Two parameter Winkler-Pasternak elastic medium is used to precisely model the elastic behavior of the matrix surrounding the nano-plate. The governing stability equations are then derived using the classical plate theory and the principle of virtual work for a perfect uniform triangular nano-plate composite system. The well-known numerical Galerkin method is then used as the basis for the solution in conjunction with the areal coordinates system. The solution procedure views the entire nano-composite plate as a single super element which can be of general shape. Effects of nonlocal parameter, length, aspect ratio, mode number, anisotropy, edge supports and elastic medium on buckling loads are investigated. All of these parameters are seen to have significant effect on the stability characteristics of nano-composite plate. It is shown that the results depend obviously on the non-locality of buckled nano-composite plate, especially at very small dimensions, small aspect ratios, higher mode numbers, higher anisotropy and stiffer edge supports. Also it is seen that the medium parameters, especially the Winkler parameter, have significant influence on the small scale effect and can decrease or increase it. Also, it is seen that the classical continuum mechanics overestimates the results which can lead to deficient design and analysis of these widely used nanostructures. The results from current study can be used in design, analysis and optimization of different nano-devices such as nano-electro-mechanical systems (NEMS) utilizing nano-composite plates as load-bearing components. Although it is seen that nano-fillers, here the nano-plates, increase the stiffness of the whole nano-composite, by increasing the bending rigidities, on the other hand it is shown in this study that the small scale effect or the nonlocal effect decreases the critical loads of the nano-composite system. Thus, the nonlocal effect plays a key role in the design of these nanostructures and must be attended and comprehensively studied to avoid the failure of the nanostructure. Further, the solution employed here is general and can be applied to nano-composite plates with arbitrary shapes which is an asset in structural optimization.

doi: 10.5829/idosi.ije.2016.29.03.16

### NOMENCLATURE

$L_1, L_2, L_3$	the areal coordinates	$[M]$	mass matrix
$A_1, A_2, A_3$	the area of the sub-triangles	$N_{xx}, N_{yy}, N_{xy}$	stress resultants
$a, b$	base side length and height of the triangular nano-plate	$\Phi_i$	trial functions
$m_0$	mass per unit area of the nano-plate	$\sigma_{ij}^{(l)}$	components of local stress tensor
$[B]$	buckling matrix	$\sigma_{ij}^{(nl)}$	components of nonlocal stress tensor
$C_i$	unknown coefficients of trial functions	$q_0$	transverse distributed pressure
$D_{ij}$	bending rigidities	$u, v, w$	displacement fields

\*Corresponding Author Email: e.raeisi@ujiroft.ac.ir (E. Raeisi Estabragh)

$E_x, E_y$	Young's modulus of nano-plate in $x$ and $y$ directions	$\mathcal{X}$	weight function
$G_{xy}$	shear modulus of the nano-plate	$\varepsilon_{ij}$	components of strain tensor
$h$	thickness of the nano-plate	$\lambda_b$	buckling parameter
$[K]$	stiffness matrix	$\mu$	nonlocal parameter
$M_{xx}, M_{yy}, M_{xy}$	moment resultants	$\nu_x, \nu_y$	Poisson's ratios in $x$ and $y$ directions
$\nabla^2$	Laplacian operator in two dimensional Cartesian coordinate system	$\rho$	density of the nano-plate
		$\omega$	circular frequency of the nano-plate

## 1. INTRODUCTION

Outstanding physical and chemical properties of nanostructures cause their wide usage in different nano-engineering systems such as nano-sensors [1], nano-actuators [2] and nano-composites [3, 4]. Among the nano-structures, the carbon nano-tubes (CNTs) and the Graphene sheets (GSs) are being vastly used in different nano-electro-mechanical systems (NEMS) and nano-composites due to their superior mechanical and electrical properties such as strength and conductivity [3-5]. Based on this, a wide range of experimental, computational and theoretical studies have been conducted on such nano-structures to comprehensively reveal their physical properties for better design and application. Among these methods, the experimental measurements, at nano scale, are hard to reproduce and depend on the development of devices for manipulation of nano-sized objects. Also, computational techniques based on semi-empirical approaches such as ab-initio [6], molecular dynamics (MD) simulation [7], density functional theory (DFT) [8], etc., which produce results in line with the experiment, are restricted by the amount of computational capacities needed for the calculations especially when the number of atoms and bonds included in the nanostructure increases. In this way, developing an appropriate theoretical model for analyzing nanostructures eliminates the difficulties associated with the previous mentioned methods while it can also produce results in agreement with them. On this basis, continuum modeling of nanostructures is being the focus of interest [9-13]. An accurate continuum model of nanostructures must take the account of change in the material and physical properties of these structures arising at the nano scale. In fact, as the dimensions of a system reduce to the nano scale, they become comparable to the inter-atomic or inter-molecular spacing of that system and the material system can no longer be modeled as a continuum. Moreover, at nano scale, the influence of long-range inter-atomic and inter-molecular cohesive forces on the static and dynamic responses tends to be significant. These effects are referred to as the "Size" or "Small scale" effects [14-16]. Since the size independent classical continuum models are unable to capture the small scale effects, the modified continuum theories

have been developed to take the account of these effects on the physical behavior of the nanostructures. Modified continuum models have the computational efficiency of the classical continuum models and at the same time produce comparable results to the experimental and semi-empirical ones. These models can be effectively used to simulate very small to very large systems. Some of the size dependent continuum theories are surface elasticity theory [17], strain gradient theory [18], couple stress theory [19] and the nonlocal elasticity theory introduced by Eringen [20, 21]. Among these theories, the nonlocal elasticity theory is seen to produce well-matched results with those from lattice, atomistic and molecular dynamics simulations [20-24]. In classical (local) continuum theory, it is assumed that stress state at a point in the continuum body depends uniquely on the strains at that point but in the nonlocal elasticity theory, it is assumed that stress state at a point depends not only on strains in that point but also on the strains at all other points of the continuum body especially on those which are in the effective neighboring domains [20, 21].

In fact, as one of the dimensions of the structure reduces to nanometer and becomes comparable to its molecular or atomic bond lengths, the small scale effects, which cause change in the physical properties, including the mechanical properties of the material, become prominent. These changes are due to the discreteness of the structures at this scale and the effect of the long-range intermolecular and interatomic cohesive forces which act on the atoms in the point under stress study from adjacent atoms or a few internal characteristic lengths further. These long-range cohesive forces induce a nonlocal effect which is captured through a cut-off function in the nonlocal continuum theory. The nonlocal elasticity theory first was used for stress analysis in crack tips and screw dislocations [20, 21]. It includes a small length scale parameter or nonlocal parameter which is obtained from matching the dispersion curves with those from lattice dynamic or atomistic/molecular simulations [20-24]. According to the Eringen [21] and other researchers using nonlocal elasticity theory [22-42], the nonlocal parameter depends on the material structure and physics of the problem under investigation e.g. loading, boundary conditions, etc.

Buckling analysis of nano scaled structures is an important issue for proper design and use of them in different nano-systems as load bearing components. There are numerous studies on the use of modified nonlocal continuum models for buckling and vibration analysis of nano-structures such as carbon nano-tubes [25], nano-beams [26], nano-rings/arches [27] and nano-plates [28-36, 43]. Among these nano-structures, nano-tubes such as CNTs and plate-like nano-structures such as GSs are widely used as reinforcement in nano-composites because of their strength and conductivity [3-5]. Different studies considering the nonlocal continuum modeling of nano-composites with such reinforcements have been conducted to examine and calibrate their buckling and vibration characteristics [28-36, 44]. In all of these studies the Eringen nonlocal elasticity theory is suggested for accurate prediction of dynamic response of equivalent continuum models of nano-plate reinforced composites and the classical theory is seen to overestimates the buckling loads.

In almost all of the studies conducted on the analysis of nano-composite plates, the shape of nano-plate has received the less attention. In this case, Duan and Wang [38] reported exact solution for axisymmetric bending of circular Graphene sheets based on the nonlocal elasticity theory. Farajpour et al. [39] reported axisymmetric buckling of circular Graphene sheets using nonlocal continuum plate model. Babaie and Shahidi [40] studied small scale effects on the buckling of quadrilateral nano plates using the Galerkin method. Malekzadeh et al. [41] investigated thermal buckling of orthotropic arbitrary straight-sided quadrilateral nano-plates using the nonlocal classical plate theory (NCPT). Anjomshoa [42] studied the buckling of elliptical nano-plates using the Ritz functions and nonlocal continuum mechanics. Ravari and Shahidi [43] also reported the buckling of annular nano-plates via finite difference method. Since the synthesis of nano-plates with controlled size and morphology is a challenging issue, a comprehensive and detailed study on the analysis of nano-plates with different shapes should be conducted to examine the load bearing capacity of these widely used nano-structures. One of these nano-plates is the triangular nano-plate which has special application in nano-engineering systems [44, 45] and can also be used as reinforcement in nano-composites. It is obvious that the exact buckling solutions are only possible for few plates with simple shapes like rectangular or circular plates under certain boundary and loading conditions. For buckling analysis of plates with arbitrary shapes, numerical methods such as finite difference method [43], finite strip method [46], differential quadrature method (DQM) [47] and Galerkin method [48-52] are usually used in the solution procedure. The Galerkin method is a well-known mesh-free numerical approximate method which is very simple to be used and manipulated for solving different kinds of plate

problem from static to dynamic [48] and linear to nonlinear [49]. These include bending [50] buckling [51] and vibration [52] of plates with arbitrary shapes. In the present work, an orthotropic nonlocal continuum model based on the classical plate theory (CPT) is developed for stability analysis of triangular nano-composite plates under uniform in-plane compression. The matrix of the composite is modeled using two-parameter Winkler-Pasternak elastic medium [53]. The principle of virtual work is used to derive the governing equations. The simultaneous eigenvalue equations are then solved using the Galerkin method on the basis of the polynomial trial functions. Effects of nonlocal parameter, length, aspect ratio, mode number, material property, different boundary conditions and medium parameters on buckling loads are thoroughly investigated. The novelty of the current work can be seen from multiple aspects including the study of decreasing effect of small scale effect in conjunction with the increasing effect of elastic medium on critical loads of nano-composite plate at higher buckling modes and the use of an efficient and easy handling numerical Galerkin's method which can be simply used for the analysis of nano-plate with arbitrary shapes and boundary conditions. Thus, current study can also be employed for buckling analysis of nano-composite plates with general shapes which makes it referable for imperfect nanostructures analysis and the structural topology optimization problem. To the best of authors' knowledge, the buckling of triangular nano-composite plates based on the nonlocal elasticity theory has not been reported in available literature.

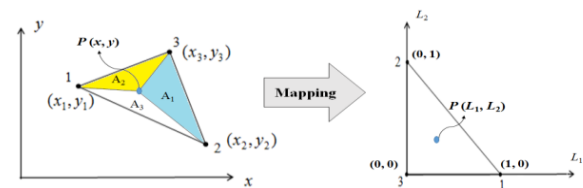


**Figure 1.** Mapping from Cartesian coordinate system to areal coordinate system.

## 2. FORMULATION

**2. 1. Geometric Definitions** An arbitrary triangle in the Cartesian coordinates  $(x, y)$  can be mapped to a right-angled triangle in the areal coordinates  $(L_1, L_2)$  with the boundary equations being as  $L_1=0$ ,  $L_2=0$  and  $L_1+L_2=1$  as shown in Figure 1. The areal coordinates  $(L_1, L_2, L_3)$  of the point P are defined as:

$$L_1 = \frac{A_1}{A} \quad L_2 = \frac{A_2}{A} \quad L_3 = \frac{A_3}{A} \quad (1)$$

where  $A_1$ ,  $A_2$  and  $A_3$  denote the areas of the sub-triangles shown in Figure 1 and  $A$  is the area of the base triangle.

The three areal coordinates are related to each other by the following expression:

$$L_1 + L_2 + L_3 = 1 \tag{2}$$

also, Cartesian and areal coordinates are related by the following relations:

$$x(L_1, L_2) = \sum_{i=1}^3 x_i L_i \tag{3.1}$$

$$y(L_1, L_2) = \sum_{i=1}^3 y_i L_i \tag{3.2}$$

where,  $x_i$  and  $y_i$  are the coordinates of vertices. Using Equations (3.1) and (3.2), the first-order and second-order derivatives, based on the areal coordinates, can be respectively expressed as:

$$\begin{Bmatrix} \frac{\partial}{\partial x} \\ \frac{\partial}{\partial y} \end{Bmatrix} = [J_{11}]^{-1} \begin{Bmatrix} \frac{\partial}{\partial L_1} \\ \frac{\partial}{\partial L_2} \end{Bmatrix} \tag{4.1}$$

$$\begin{Bmatrix} \frac{\partial^2}{\partial x^2} \\ \frac{\partial^2}{\partial y^2} \\ \frac{\partial^2}{\partial x \partial y} \end{Bmatrix} = [J_{22}]^{-1} \tag{4.2}$$

$$\begin{pmatrix} \frac{\partial^2}{\partial L_1^2} \\ \frac{\partial^2}{\partial L_2^2} \\ \frac{\partial^2}{\partial L_1 \partial L_2} \end{pmatrix} = [J_{21}][J_{11}]^{-1} \begin{Bmatrix} \frac{\partial}{\partial L_1} \\ \frac{\partial}{\partial L_2} \end{Bmatrix} \tag{4.2}$$

where,  $[J_{11}]$ ,  $[J_{21}]$  and  $[J_{22}]$  are the mapping matrices defined as:

$$[J_{11}] = \begin{bmatrix} \frac{\partial x}{\partial L_1} & \frac{\partial y}{\partial L_1} \\ \frac{\partial x}{\partial L_2} & \frac{\partial y}{\partial L_2} \end{bmatrix} \tag{5.1}$$

$$[J_{21}] = \begin{bmatrix} \frac{\partial^2 x}{\partial L_1^2} & \frac{\partial^2 y}{\partial L_1^2} \\ \frac{\partial^2 x}{\partial L_2^2} & \frac{\partial^2 y}{\partial L_2^2} \\ \frac{\partial^2 x}{\partial L_1 \partial L_2} & \frac{\partial^2 y}{\partial L_1 \partial L_2} \end{bmatrix} \tag{5.2}$$

$$[J_{22}] = \begin{bmatrix} \left(\frac{\partial x}{\partial L_1}\right)^2 & \left(\frac{\partial y}{\partial L_1}\right)^2 & 2\left(\frac{\partial x}{\partial L_1}\right)\left(\frac{\partial y}{\partial L_1}\right) \\ \left(\frac{\partial x}{\partial L_2}\right)^2 & \left(\frac{\partial y}{\partial L_2}\right)^2 & 2\left(\frac{\partial x}{\partial L_2}\right)\left(\frac{\partial y}{\partial L_2}\right) \\ \left(\frac{\partial x}{\partial L_1}\right)\left(\frac{\partial x}{\partial L_2}\right) & \left(\frac{\partial y}{\partial L_1}\right)\left(\frac{\partial y}{\partial L_2}\right) & \left(\frac{\partial x}{\partial L_1}\right)\left(\frac{\partial y}{\partial L_2}\right) + \left(\frac{\partial y}{\partial L_1}\right)\left(\frac{\partial x}{\partial L_2}\right) \end{bmatrix} \tag{5.3}$$

**2. 2. Nonlocal Classical Plate Theory** Discrete and nonlocal continuum models of a typical triangular nano-composite plate, here the Graphene based nano-composite, under uniform in-plane compression are shown in Figure 2. Cartesian coordinate system is chosen for deriving the governing equations with its origin being fixed at the center of the mid-plane. The displacement fields at the time  $t$  according to classical plate theory (CPT) are written as:

$$\begin{aligned} u(x, y, t) &= u_0(x, y, t) - z w_{,x}(x, y, t), \\ v(x, y, t) &= v_0(x, y, t) - z w_{,y}(x, y, t), \\ w(x, y, t) &= w(x, y, t) \end{aligned} \tag{6}$$

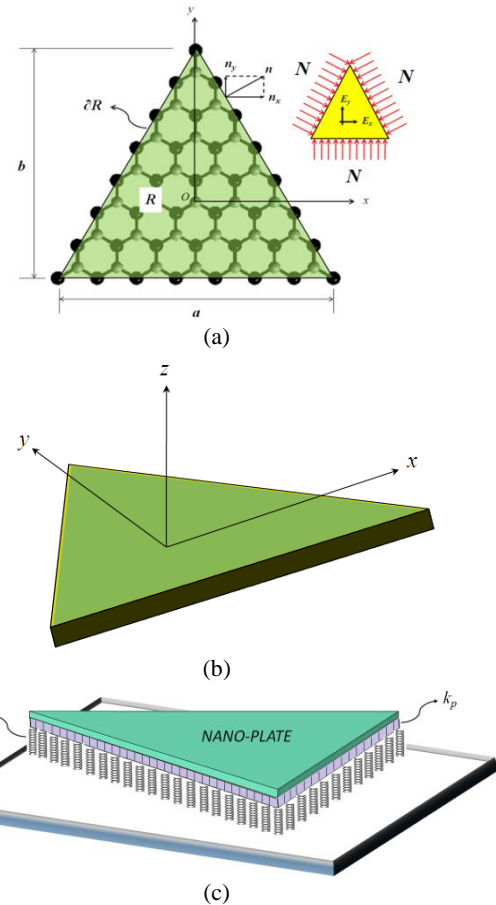


**Figure 2.** Triangular nano-composite plate under in-plane uniform compression: (a) discrete model; (b) continuum model; (c) two-parameter model of elastic medium.

Here,  $u_0$ ,  $v_0$  and  $w$  denote displacement of the point  $(x,y,0)$  along  $x$ ,  $y$  and  $z$  directions, respectively. The strain components are then obtained as:

$$\begin{aligned} \varepsilon_{xx} &= u_{0,x} - zW_{,xx}, \quad \varepsilon_{yy} = v_{0,y} - zW_{,yy}, \\ \varepsilon_{xy} &= \frac{1}{2}(u_{0,y} + v_{0,x} - 2zW_{,xy}) \\ \varepsilon_{zz} &= \varepsilon_{xz} = \varepsilon_{yz} = 0 \end{aligned} \tag{7}$$

According to Eringen [20, 21], the nonlocal behavior of a Hookean solid can be introduced by the following differential constitutive equations:

$$\begin{aligned} \sigma^{(nl)} - \alpha l_e^2 \nabla^2 \sigma^{(nl)} &= \sigma^{(l)} = \mathbf{S}\varepsilon, \\ \alpha &= \left( \frac{e_0 l_i}{l_e} \right)^2 \end{aligned} \tag{8}$$

Here,  $\nabla^2(\bullet) = (\bullet)_{,xx} + (\bullet)_{,yy}$  is the Laplacian operator in two dimensional Cartesian coordinate system. Also,  $\sigma^{(l)}$ ,  $\sigma^{(nl)}$ ,  $\mathbf{S}$  and  $\varepsilon$  are, respectively, the local stress tensor, the nonlocal stress tensor, the elasticity tensor and the strain tensor, defined as:

$$\begin{aligned} \sigma^{(l)} &= \begin{Bmatrix} \sigma_{xx}^{(l)} \\ \sigma_{yy}^{(l)} \\ \sigma_{xy}^{(l)} \end{Bmatrix}, \quad \sigma^{(nl)} = \begin{Bmatrix} \sigma_{xx}^{(nl)} \\ \sigma_{yy}^{(nl)} \\ \sigma_{xy}^{(nl)} \end{Bmatrix}, \\ \mathbf{S} &= \begin{bmatrix} \frac{E_x}{1-\nu_x \nu_y} & \frac{\nu_x E_y}{1-\nu_x \nu_y} & 0 \\ \frac{\nu_y E_x}{1-\nu_x \nu_y} & \frac{E_y}{1-\nu_x \nu_y} & 0 \\ 0 & 0 & G_{xy} \end{bmatrix}, \quad \varepsilon = \begin{Bmatrix} \varepsilon_{xx} \\ \varepsilon_{yy} \\ 2\varepsilon_{xy} \end{Bmatrix} \end{aligned} \tag{9}$$

In Equation (8),  $\alpha$  represents the small scale parameter which depends on a characteristic length ratio  $l_i/l_e$  in which  $l_i$  is an internal characteristic length which can be lattice parameter, size of grain, granular distance or distance between C-C bonds in carbon nano-structures such as CNTs and GSs and  $l_e$  is an external characteristic length which can be wavelength, crack length or one of the dimensions of the nanostructure. The parameter  $e_0$  is a material constant related to the structure of the nano-plate and should be determined for each material independently from matching nonlocal continuum results with atomistic ones. It is obvious that Equation (8) for  $\alpha=0$  yields the well-known classical constitutive equations of the elastic solids. Based on Equation (9), the following stress and moment resultants can be defined:

$$\begin{aligned} \mathbf{N} &= \int_{-\frac{h}{2}}^{\frac{h}{2}} \sigma^{(nl)} dz, \quad \mathbf{M} = \int_{-\frac{h}{2}}^{\frac{h}{2}} z \sigma^{(nl)} dz, \\ \mathbf{N} &= \begin{Bmatrix} N_{xx} \\ N_{yy} \\ N_{xy} \end{Bmatrix}, \quad \mathbf{M} = \begin{Bmatrix} M_{xx} \\ M_{yy} \\ M_{xy} \end{Bmatrix} \end{aligned} \tag{10}$$

where,  $h$  denotes the nano-plate's thickness. According to Equation (8), the nonlocal effect enters through the constitutive relations. Since, the principle of virtual

work is independent of the constitutive relations it can be employed to derive the equilibrium equations for the current nonlocal plate model. After applying this principle the equations of motion are obtained as [31]:

$$N_{xx,x} + N_{xy,y} = m_0 \ddot{u} \tag{11.1}$$

$$N_{xy,x} + N_{yy,y} = m_0 \ddot{v} \tag{11.2}$$

$$\begin{aligned} M_{xx,xx} + 2M_{xy,xy} + M_{yy,yy} &+ (N_{xx} w_{,x})_{,x} \\ &+ (N_{yy} w_{,y})_{,y} + (N_{xy} w_{,y})_{,x} + (N_{yx} w_{,x})_{,y} \\ &+ q_0 - m_0 \ddot{w} + m_2 (\ddot{w}_{,xx} + \ddot{w}_{,yy}) = 0 \end{aligned} \tag{11.3}$$

here,  $m_0$  and  $m_2$  are, respectively, mass per unit of area and mass moment of inertia of the nano-plate defined as:

$$m_0 = \int_{-\frac{h}{2}}^{\frac{h}{2}} \rho dz, \quad m_2 = \int_{-\frac{h}{2}}^{\frac{h}{2}} \rho z^2 dz \tag{12}$$

where,  $\rho$  denotes the density of nano-plate. In Equation (11.3)  $q_0$  is the external applied transverse load which here is exerted by the elastic medium and then is defined as:

$$q_0 = -k_w w + k_p (w_{,xx} + w_{,yy}) \tag{13}$$

where,  $k_w$  is the Winkler parameter which represents the springy effect of the elastic medium by modelling it as a series of condensed linear springs. Also, in the above equation,  $k_p$  is the Pasternak parameter of the elastic medium and represents the shear interaction between the nano-plate and the elastic medium attached to it. As it is seen in the above equation, in the current model of elastic medium, the exerted pressure on the nano-plate is proportional to the transverse deflection and curvatures of the nano-plate (linear elastic medium). Using Equations (7)-(10) and assuming the two dimensional Laplacian operation, the moment resultants can be expressed in terms of the displacement field as:

$$\mathbf{M} - \mu \nabla^2 \mathbf{M} = -\mathbf{D}\kappa \tag{14}$$

here  $\mu = (e_0 l_i)^2$  is the nonlocal parameter,  $\mathbf{D}$  is the bending rigidity tensor and  $\kappa$  is the curvature vector of the nano-plate defined as:

$$\mathbf{D} = \frac{h^3}{12} \mathbf{S}, \quad \kappa = \langle w_{,xx} \quad w_{,yy} \quad 2w_{,xy} \rangle^T \tag{15}$$

Using Equations (11.3), (13) and (14) and assuming the solution  $w(x, y, t) = W(x, y) \exp(i\omega t)$ , the following governing equation will be obtained for the nonlocal plate model of nano-composite in terms of transverse displacement [28, 31, 41]:

$$\begin{aligned}
 &D_{11}W_{,xxxx} + 2(D_{12} + 2D_{33})W_{,xyyy} + D_{22}W_{,yyyy} \\
 &-(1 - \mu\nu^2)\left[-k_w w + k_p (w_{,xx} + w_{,yy}) + m_0 \omega^2 W \right. \\
 &-m_2 \omega^2 (W_{,xx} + W_{,yy}) + (N_{xx} W_{,x})_{,x} + (N_{yy} W_{,y})_{,y} \\
 &\left. + (N_{xy} W_{,y})_{,x} + (N_{yx} W_{,x})_{,y}\right] = 0
 \end{aligned} \tag{16}$$

where,  $W$  denotes the deflection of the nano-plate middle surface and  $\omega$  is the natural circular frequency.

### 3. SOLUTION PROCEDURE

Applying the weighted residual method to the governing equation in Equation (17) gives:

$$\iint_R \left\{ D_{11}W_{,xxxx} + 2(D_{12} + 2D_{33})W_{,xyyy} + D_{22}W_{,yyyy} - (1 - \mu\nu^2)\left[-k_w w + k_p (w_{,xx} + w_{,yy}) + m_0 \omega^2 W \right. \right. \\
 \left. \left. -m_2 \omega^2 (W_{,xx} + W_{,yy}) + (N_{xx} W_{,x})_{,x} + (N_{yy} W_{,y})_{,y} + (N_{xy} W_{,y})_{,x} + (N_{yx} W_{,x})_{,y}\right] \right\} \chi dx dy = 0 \tag{17}$$

where,  $\chi$  denotes the weight function. Using the divergence theorem the following form will be reached:

$$\iint_R \Pi(x, y) dx dy + \int_{\partial R} \Lambda(s) ds = 0 \tag{18}$$

where,  $\Pi$  and  $\Lambda$  are given in Appendix (A.1 and A.2). Also,  $R$  is the area of the nano-plate,  $\partial R$  represents the boundary of the nano-plate and  $\langle n_x \ n_y \rangle$  are the components of the unit normal vector on the boundary of the nano-plate shown in Figure 1a. For simply supported and clamped edges, the boundary conditions are simply supported edge:

$$\begin{aligned}
 &W = 0, \text{ and} \\
 &M_{nn} = n_x^2 M_{xx} + 2n_x n_y M_{xy} + n_y^2 M_{yy} = 0
 \end{aligned} \tag{19}$$

Clamped edge:

$$W = 0, \text{ and } W_{,n} = n_x W_{,x} + n_y W_{,y} = 0 \tag{20}$$

An approximate solution of the problem can be obtained by assuming an expression for the transverse deflection of the mid-surface which satisfies the essential boundary condition at the edges as:

$$W(L_1, L_2) = \sum_{q=0}^p \sum_{r=0}^q C_i \Phi_i(L_1, L_2) \tag{21}$$

In which,  $C_i$  are the unknown coefficients to be varied and  $\Phi_i$  are defined as:

$$\Phi_i = [L_1 L_2 L_3]^k \varphi_i(L_1, L_2) \tag{22}$$

In the above equation,  $k$  is the power of the geometrical shape equation which takes 1 and 2 for simply supported and clamped edges, respectively. On this way, Equation (21) satisfies the kinematical boundary conditions at the edges. Also,  $\varphi_i$  are polynomial trial functions of the form:

$$\varphi_i(L_1, L_2) = L_1^{q-r} L_2^r \tag{23}$$

where:

$$i = \frac{(q+1)(q+2)}{2} - r \tag{24}$$

In Equation (21),  $p$  is the degree of polynomial set which may be increased until the desired accuracy is achieved. Substituting Equation (21) into Equation (18) and using the Galerkin method assumption i.e.  $\chi = \Phi_i$ , the following simultaneous linear equations for both vibration and buckling problems will be yielded:

$$([K] - \beta_1 \omega^2 [M] - \beta_2 N_{xx} [B]) \{C\} = \{0\} \tag{25}$$

In which,  $[K]$ ,  $[M]$  and  $[B]$ , defined in Appendix A, are respectively the stiffness, mass and buckling matrices associated with the nano plate. The scalar indicators  $\beta_j$  take on  $\beta_1=1, \beta_2=0$  for free vibration problem and  $\beta_1=0, \beta_2=1$  for the buckling problem. For simplicity the results are presented in non-dimensional buckling load parameter as  $\lambda_b = |N_{xx}|a^2/D_{11}$ . In the case of uniform in-plane compression in Figure 2a we have:

$$N_{xx} = N_{yy} = -N, \quad N_{xy} = 0 \tag{26}$$

Equation (25) is a standard eigenvalue problem which can be solved for critical frequencies or buckling loads of triangular nano-composite plates with the corresponding eigenvector  $\{C\}$  which represents the associated vibration or buckling mode shape.

## 4. RESULTS AND DISCUSSIONS

**4. 1. Validation and Convergence** In order to establish the validation of the current work, buckling loads for simply supported and clamped isotropic isosceles triangular plates with Young's modulus 1.06Tpa, Poisson's ratio 0.3, mass density 2.3 g/cm<sup>3</sup> and thickness  $h=0.34$  nm are calculated from Equation (25) and are compared in Table 1. A comparison in Table 1 shows desired agreement between the results obtained here and those reported by Wang and Liew [54]. Another convergence study is also performed in Table 2 for the nonlocal case. From Tables 1 and 2 it is found that a polynomial set of degree  $p=10$  is sufficient for the convergence of the results and the set is used to generate all the other results presented herein.

**4. 2. Effect of Nonlocal Parameter, Size and Mode Number** In this section the small scale effect on critical loads of isosceles triangular nano-plate is investigated for different values of base side length, aspect ratio and mode number. The base side length of the nano-plate is varied between 5nm and 35nm and the range of aspect ratio is considered to increase from 1 to 3.

**TABLE 1.** Convergence study of buckling parameter  $\lambda_b$  for local ( $\mu=0$ ) continuum model of isosceles triangular nano-plate

Degree of polynomial set (p)	Aspect ratio (b/a)				
	1	1.5	2	2.5	3
Simply supported (SSS)					
4	45.8309	32.8100	27.0040	23.6718	21.6069
6	45.8274	32.7266	26.9092	23.6190	21.5031
8	45.8273	32.7250	26.9068	23.6137	21.4855
10	45.8273	32.7248	26.9064	23.6131	21.4846
Ref [54]	45.827	32.725	26.906	23.613	21.484
Clamped (CCC)					
4	127.6994	92.7763	77.5437	69.8652	65.5726
6	127.6104	92.3908	77.2715	69.0510	63.7749
8	127.6095	92.3770	77.2517	68.8900	63.5719
10	127.6094	92.3767	77.2506	68.8812	63.5646
Ref [54]	127.610	92.377	77.251	68.881	63.564

**TABLE 2.** Convergence study of buckling parameter  $\lambda_b$  for nonlocal continuum model of isosceles triangular nano-plate ( $b/a=2, a=10$  nm)

Degree of polynomial set (p)	Nonlocal parameter ( $\mu$ )				
	0	1	2	3	4
Simply supported (SSS)					
4	27.0040	21.2623	17.5342	14.9184	12.9817
6	26.9092	21.2035	17.4941	14.8894	12.9597
8	26.9068	21.2020	17.4931	14.8886	12.9592
10	26.9064	21.2017	17.4929	14.8885	12.9591
Clamped (CCC)					
4	77.5437	43.6758	30.3989	23.3122	18.9050
6	77.2715	43.5894	30.3570	23.2876	18.8888
8	77.2517	43.5831	30.3539	23.2858	18.8876
10	77.2506	43.5827	30.3537	23.2857	18.8876

The nonlocal parameter is also assumed to vary between  $\mu=0$  nm<sup>2</sup> and 4 nm<sup>2</sup>. Firstly, the influence of base side length and nonlocal parameter on buckling loads are illustrated by Figure 3 for  $b/a=1$ . From this figure it is found that nonlocal critical buckling loads are smaller than the local ones ( $\mu=0$ ). In addition, for each value of the base side length, by increasing the nonlocal parameter the buckling loads decrease. The reason is that when the nonlocal parameter increases, the small scale effects increases and this leads to a reduction in the nano-plate stiffness [31]. In fact, the nonlocal effect decreases the nano-plate buckling resistance of nano-plate by increasing the intensity of buckling matrix through the nonlocal terms in Equation (25). It is also seen in Figure 3 that by increasing the base side length, the nonlocal effect decreases and the buckling loads converge to the local ones. This implies that by increasing the external characteristic length of the nano-plate (here the base side length of nano-plate  $a$ ) the small scale effect decreases while the internal characteristic length is assumed to be unchanged. This

is due to the size dependency in the essence of the nonlocal elasticity theory which states that as the system becomes larger, become closer to the classical continuum size order, the nonlocal or small scale effect disappears [31, 38-42]. For better understanding the influence of the base side length and nonlocal parameter, the relative errors, in percentage form, due to neglecting the nonlocal effect for base side lengths  $a=10$ nm and  $a=30$ nm with the nonlocal parameter  $\mu=4$  nm<sup>2</sup>, are found to be 51.83% and 10.68%, respectively. It is found from these values that for large enough nano-structures the classical continuum modelling can be desirably employed instead of the more complicated nonlocal theory. Here and afterwards, the relative error is defined as  $(|Local\ result - Nonlocal\ result|)/(|Local\ result|)$ .

To see the effect of aspect ratio, the buckling parameters are plotted in Figure 4 against the aspect ratio ( $b/a$ ) for different nonlocal parameters. Here the base side length  $a=10$  nm is taken. It is found from this figure that for small aspect ratios, the difference

between nonlocal and local results is more prominent. An interpretation for such result is that for a specific value of the base side length and nonlocal parameter, as the aspect ratio increases the nano-plate become larger and this leads to a decrease in the small scale effect due to the previously discussed size dependent nature of the nonlocal elasticity theory. The relative error for ratios  $b/a=1$  and  $b/a=3$  with  $\mu=4 \text{ nm}^2$  are obtained as 64.70 and 46.22%, respectively. Thus, it is concluded that the nonlocal theory should be considered for the buckling analysis of triangular nano-plate with small aspect ratios.

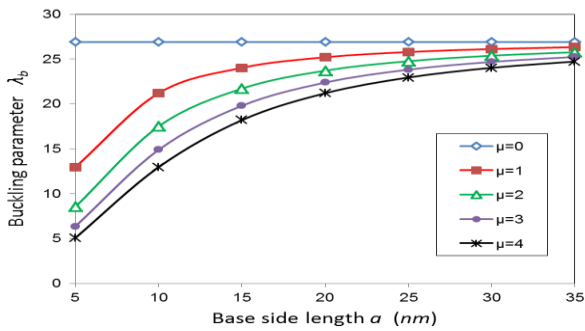


**Figure 3.** Variation of the buckling parameter with base side length of fully simply supported (SSS) isosceles triangular nano-plate for different nonlocal parameters

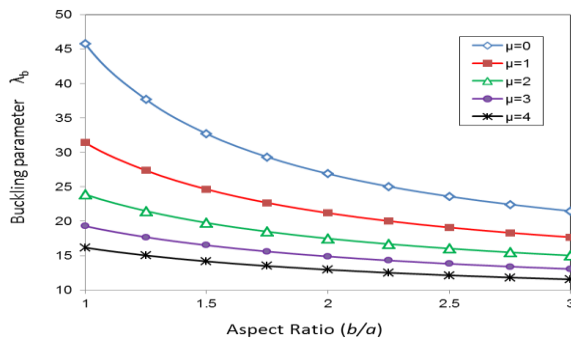


**Figure 4.** Variation of the buckling parameter with aspect ratio for different nonlocal parameters (SSS)

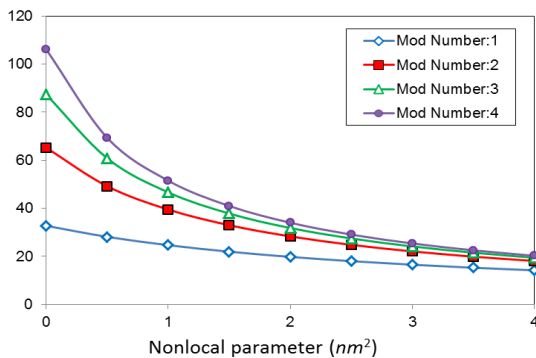


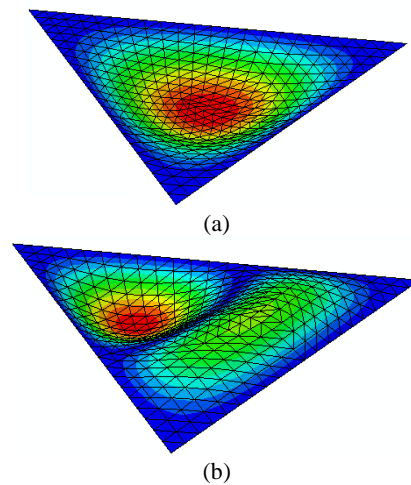
**Figure 5.** Variations of the buckling loads parameter with small scale effect for the first four buckling modes (SSS)

To study the small scale effect in different buckling modes, non-dimensional buckling loads associated with the first four mode numbers are depicted in Figure 5 for different nonlocal parameters. Here, the base side length and aspect ratio are taken as  $a=10 \text{ nm}$ ,  $b/a=1.5$ , respectively.

It can be seen in the figure that in all of the mode numbers as the nonlocal parameter increases the buckling parameter decreases. Further, it is revealed that the nonlocal effect is more prominent in higher mode numbers. This is also true for a circular nano-plate under uniform compression [39]. For the nonlocal parameter  $\mu=4 \text{ nm}^2$  the relative error due neglecting the small scale effect for the first and fourth mode numbers are obtained as 56.67% and 80.94%, respectively. The buckling loads associated with the first four modes for a right-angled triangular nano-plate are, as well, presented in Table 3. It is seen in this table that similar to isosceles triangular nano-plate (Figure 5) the buckling loads of right-angled triangular nano-plate also decrease by nonlocal parameter in all modes. The associated buckling mode shapes for the isosceles and the right-angled triangular nano-plates are presented in Figure 6 and Figure 7, respectively.

**4. 3. Effect of Material Properties**

An investigation is performed to account for the effect of anisotropy in the orthotropic case. For this purpose, variations of the non-dimensional critical loads for a fully simply supported isosceles triangular nano-plate with aspect ratio  $b/a=1$  are plotted in Figure 8 against the anisotropy ratio  $E_y/E_x$  for different nonlocal parameters. The figure shows that anisotropy has an increasing effect on the critical buckling loads and as the nonlocal parameter increases this occurs in a more nonlinear manner. Also, it can be seen that as the anisotropy ratio increases the difference between local and nonlocal results increases.





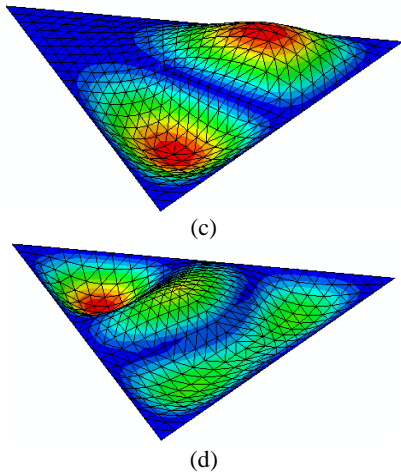


**Figure 6.** Buckling mode shapes of isosceles triangular nano-plate: (a) 1st mode; (b) 2nd mode; (c) 3rd mode; (d) 4th mode

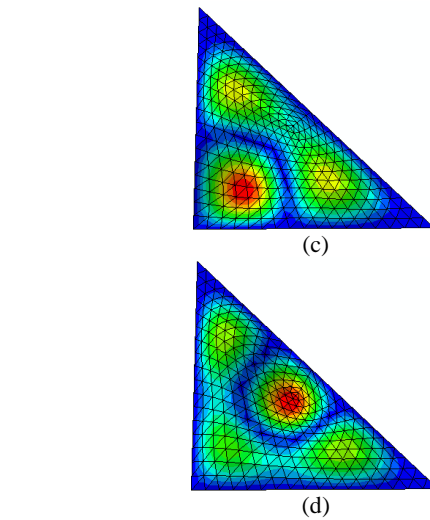
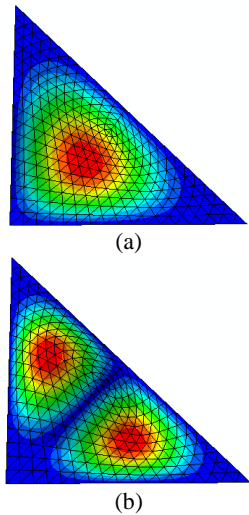


**Figure 7.** Buckling mode shapes of right-angled triangular nano-plate: (a) 1st mode; (b) 2nd mode; (c) 3rd mode; (d) 4th mode

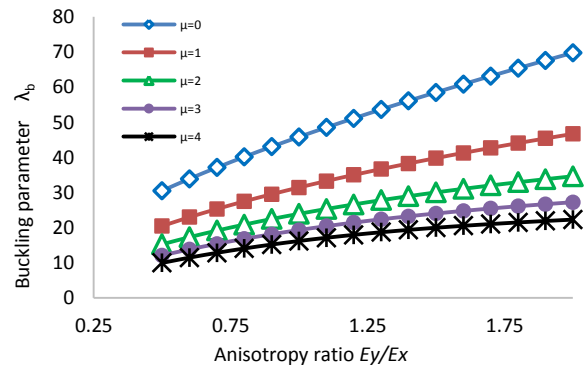


**Figure 8.** Variations of buckling parameter with anisotropy ratio for different nonlocal parameters

**TABLE 3.** Buckling parameter  $\lambda_b$  in the first four buckling modes for nonlocal plate model of right-angled triangular nano-plate ( $b/a=1, a=10$  nm)

Buckling mode	Nonlocal parameter $\mu$				
	0	1	2	3	4
Simply supported (SSS)					
1st	49.3480 (49.348)	33.0423	24.8359	19.8949	16.5936
2 <sup>nd</sup>	98.6994	49.6727	33.1876	24.9179	19.9474
3rd	128.3193	56.2017	35.9802	26.4599	20.9235
4th	167.8318	62.6631	38.5233	27.8100	21.7588
Clamped (CCC)					
1st	139.5749 (139.57)	58.2594	36.8126	26.9073	21.2023
2nd	205.5739	67.2747	40.2181	28.6825	22.2894
3rd	247.8953	71.2557	41.6078	29.3824	22.7097
4th	304.7242	75.2918	42.9523	30.0466	23.1045

\* Values in parentheses are taken from [54].

**4. 4. Effect of Edge Supports** The effect of small scale on the buckling loads of an isosceles triangular nano-plate is shown in Figure 9 for different support conditions at edges. It is seen in the figure that in both fully simply supported (SSS) and fully clamped boundary conditions (CCC), as the nonlocal parameter increases the buckling load parameter decreases. Further, it is found that the nonlocal effect is more prominent for clamped boundary condition. The relative error percent due to neglecting nonlocal effect for fully simply supported and fully clamped edges with  $\mu=4\text{nm}^2$  are found to be 51.83% and 75.55%, respectively.

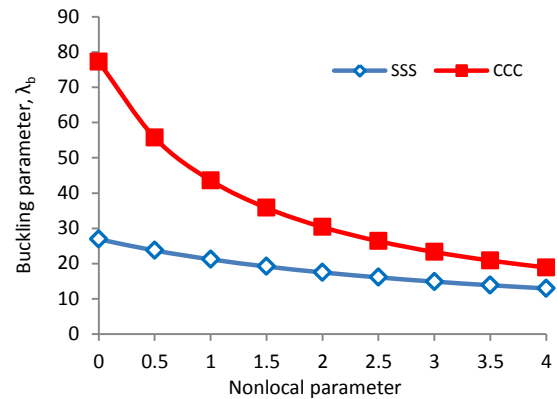
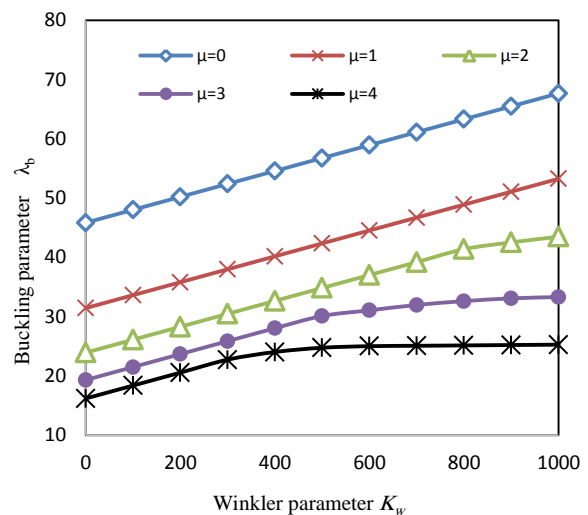
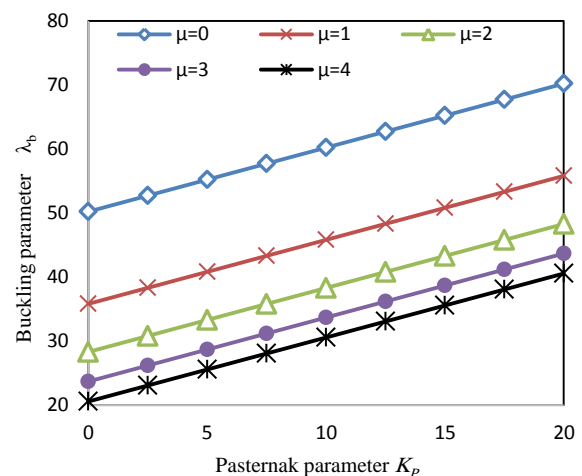


**Figure 9.** Effect of edges support and nonlocal parameter on buckling parameter

**4. 5. Effect of Elastic Medium** As the nano-plates are used as reinforcements in advanced nano-composites [3-5], an investigation on the effect of elastic medium on critical loads of a triangular nano-composite plate, in the presence of non-locality, is carried out in this section. Since the elastic matrix of nano-composite here is modeled using the two-parameter Winkler-Pasternak elastic medium, Equation (13), the effect of these parameters namely the Winkler parameter  $k_w$  and the Pasternak parameter  $k_p$  on critical buckling loads are studied and the results are presented in Figure 10a and Figure 10b, respectively. It is seen in Figure 10a that as the Winkler parameter increases the buckling loads increase for all values of nonlocal parameter. Also it is found in this figure that as the nonlocal parameter increases the current increase takes place in a nonlinear manner. The Pasternak parameter of the medium has the same influence on the buckling parameter as it can be seen in Figure 10b. However, here in the current domain of the Pasternak parameter, the increase in buckling parameter is linear. It is seen that the medium parameters affect the influence of nonlocal parameter on the results as was reported before [31].



(a)



(b)

**Figure 10.** Effect of elastic medium and nonlocal parameter on critical buckling loads of isosceles triangular nano-composite plate: (a) Winkler parameter; (b) Pasternak parameter.

To show this, error percent form of the results are presented in Figure 11a and 11b for Winkler and Pasternak parameters, respectively. It is found from Figure 11a that for nonlocal parameter  $\mu=1 \text{ nm}^2$  as the Winkler parameter increases the error percent decreases. This means that the increase in Winkler parameter of elastic medium, a harder matrix for nano-composite plate, decreases the nonlocal effect for the current value of nonlocal parameter. But for other nonlocal parameters the trend is somehow different. For example for nonlocal parameter  $\mu=2 \text{ nm}^2$  the error percent decreases by Winkler parameter until a special amount, here about  $K_w=800$ , then it increases with Winkler parameter. This can be interpreted so that as the medium become stiffer the nano-composite plate buckles in a different mode shape, a higher mode, and as the nonlocal effect is more prominent in the higher buckling modes, as discussed in section 4.2, the error percent increases.

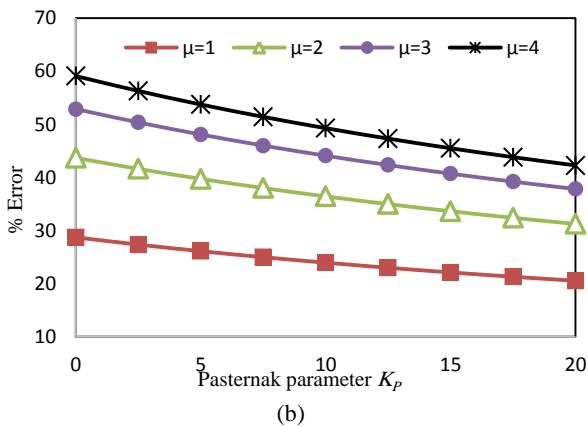
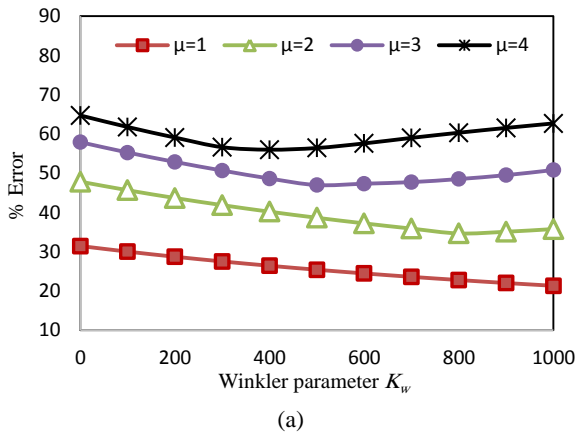


**Figure 11.** Effect of elastic medium on the influence of nonlocal parameter on critical buckling loads of isosceles triangular nano-composite plate: (a) Winkler parameter; (b) Pasternak parameter.

In fact, the magnitude of Winkler parameter of elastic medium affects the buckling mode shape. Further, from Figure 11a it is revealed that as the nonlocal parameter increases this change in the error percent or change in buckling mode occurs for smaller Winkler parameters. For better understanding, the change in buckling mode shape with Winkler parameter is presented in Figure 12. From Figure 11b, also, it is found that as the Pasternak parameter increases the error percent and the nonlocal effect decrease. In fact, in the current domain for the Pasternak parameter the buckling mode shape is the same and the variation of error percent are smooth and linear. Thus, based on this interpretation the nonlinear manner in Figure 10a is also well understood. It should be noted that in Figures 10a, 10b, 11a and 11b the results are presented for non-dimensional medium parameters which are defined as:

$$K_w = \frac{k_w a^4}{D_{11}}, \quad K_p = \frac{k_p a^2}{D_{11}}. \quad (27)$$

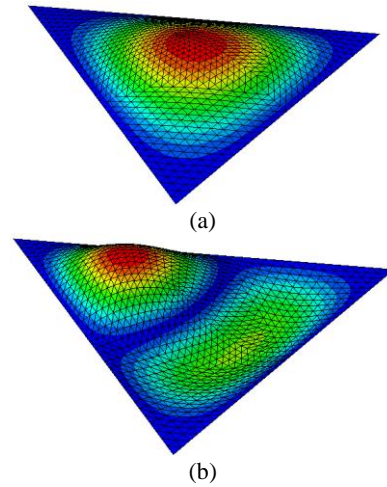


**Figure 12.** Buckled isosceles triangular nano-composite plate with nonlocal parameter  $\mu=2\text{nm}^2$ : (a)  $K_w=800$ ; (b)  $K_w=900$ .

### 5. CONCLUSION

In this work, buckling analysis of orthotropic triangular nano-composite plates under uniform in-plane compression at the nano scale has been studied using the nonlocal CPT. Based on the nonlocal theory, the governing equations for both vibration and buckling problems have been derived and the Galerkin method has been applied to solve the eigenvalue equations. Areal coordinates system has been employed to express the geometry of triangular nano-composite plate with arbitrary shape in a simple form, and then the interpolation functions have been used to form an assumed expression for the transverse displacement which also satisfies the kinematic boundary conditions at the edges. In the current solution method, there is no need for mesh generation and thus large degrees of freedoms. Effect of small scale for different base side lengths, mode numbers, aspect ratios, material parameters, boundary conditions and medium parameters has been investigated. From the study the following conclusions can be drawn:

- The small scale has a decreasing effect on the critical loads of isosceles and right-angled triangular nano-composite plates.
- Nonlocal effect becomes more prominent when the base side length of triangular nano-composite plate decreases.
- The small scale effect decreases when the aspect ratio increases.
- Non-locality has greater influence on critical loads in higher mode numbers.
- Buckling parameter increases by increasing degree of anisotropy and the difference between nonlocal and local results increases for greater values of anisotropy ratio.

- The nonlocal effect is more prominent for clamped edges.
- The Winkler parameter of elastic matrix increases the critical loads of triangular nano-composite plates but has different influences on the nonlocal effect i.e. it can decrease or increase the nonlocal effect depending on its value and the buckled shape of the nano-composite plate.
- The Pasternak parameter of the medium increases the buckling loads of the triangular nano-composite plate and decreases the nonlocal effect both in linear manners.

Finally, it has to be mentioned that the solution procedure taken here can also be applied for the buckling analysis of nano-composite plates with arbitrary shape which is an efficiency for imperfect structures' analysis and topology optimization problems in which other methods of studying such as experiment or molecular simulations may be impossible or lead to huge time lapses.

## 6. REFERENCE

1. Cui, Y., Wei, Q., Park, H. and Lieber, C.M., "Nanowire nanosensors for highly sensitive and selective detection of biological and chemical species", *Science*, Vol. 293, No. 5533, (2001), 1289-1292.
2. Yao, J.J., Arney, S.C. and MacDonald, N.C., "Fabrication of high frequency two-dimensional nanoactuators for scanned probe devices", *Journal of Microelectromechanical Systems*, Vol. 1, No. 1, (1992), 14-22.
3. Moniruzzaman, M. and Winey, K.I., "Polymer nanocomposites containing carbon nanotubes", *Macromolecules*, Vol. 39, No. 16, (2006), 5194-5205.
4. Ramanathan, T., Abdala, A., Stankovich, S., Dikin, D., Herrera-Alonso, M., Piner, R., Adamson, D., Schniepp, H., Chen, X. and Ruoff, R., "Functionalized graphene sheets for polymer nanocomposites", *Nature Nanotechnology*, Vol. 3, No. 6, (2008), 327-331.
5. Grossiord, N., Loos, J., Regev, O. and Koning, C.E., "Toolbox for dispersing carbon nanotubes into polymers to get conductive nanocomposites", *Chemistry of Materials*, Vol. 18, No. 5, (2006), 1089-1099.
6. Van Lier, G., Van Alsenoy, C., Van Doren, V. and Geerlings, P., "Ab initio study of the elastic properties of single-walled carbon nanotubes and graphene", *Chemical Physics Letters*, Vol. 326, No. 1, (2000), 181-185.
7. Jiang, J.-W., Wang, J.-S. and Li, B., "Young's modulus of graphene: A molecular dynamics study", *Physical Review B*, Vol. 80, No. 11, (2009).
8. Topsakal, M. and Ciraci, S., "Elastic and plastic deformation of graphene, silicene, and boron nitride honeycomb nanoribbons under uniaxial tension: A first-principles density-functional theory study", *Physical Review B*, Vol. 81, No. 2, (2010).
9. Behfar, K., Seifi, P., Naghdabadi, R. and Ghanbari, J., "An analytical approach to determination of bending modulus of a multi-layered graphene sheet", *Thin Solid Films*, Vol. 496, No. 2, (2006), 475-480.
10. Heireche, H., Tounsi, A., Benhassaini, H., Benzair, A., Bendahmane, M., Missouri, M. and Mokadem, S., "Nonlocal elasticity effect on vibration characteristics of protein microtubules", *Physica E: Low-dimensional Systems and Nanostructures*, Vol. 42, No. 9, (2010), 2375-2379.
11. Tounsi, A., Heireche, H., Berrabah, H., Benzair, A. and Boumia, L., "Effect of small size on wave propagation in double-walled carbon nanotubes under temperature field", *Journal of Applied Physics*, Vol. 104, No. 10, (2008)..
12. Aydogdu, M., "Axial vibration analysis of nanorods (carbon nanotubes) embedded in an elastic medium using nonlocal elasticity", *Mechanics Research Communications*, Vol. 43, No., (2012), 34-40.
13. Aydogdu, M., "A general nonlocal beam theory: Its application to nanobeam bending, buckling and vibration", *Physica E: Low-dimensional Systems and Nanostructures*, Vol. 41, No. 9, (2009), 1651-1655.
14. Sorop, T. and de Jongh, L., "Size-dependent anisotropic diamagnetic screening in superconducting sn nanowires", *Physical Review B*, Vol. 75, No. 1, (2007).
15. Benguediab, S., Tounsi, A., Zidour, M. and Semmah, A., "Chirality and scale effects on mechanical buckling properties of zigzag double-walled carbon nanotubes", *Composites Part B: Engineering*, Vol. 57, (2014), 21-24.
16. Chang, T. and Gao, H., "Size-dependent elastic properties of a single-walled carbon nanotube via a molecular mechanics model", *Journal of the Mechanics and Physics of Solids*, Vol. 51, No. 6, (2003), 1059-1074.
17. Gurtin, M.E. and Murdoch, A.I., "A continuum theory of elastic material surfaces", *Archive for Rational Mechanics and Analysis*, Vol. 57, No. 4, (1975), 291-323.
18. Lam, D.C.C., Yang, F., Chong, A., Wang, J. and Tong, P., "Experiments and theory in strain gradient elasticity", *Journal of the Mechanics and Physics of Solids*, Vol. 51, No. 8, (2003), 1477-1508.
19. Toupin, R.A., "Theories of elasticity with couple-stress", *Archive for Rational Mechanics and Analysis*, Vol. 17, No. 2, (1964), 85-112.
20. Eringen, A.C., "Linear theory of nonlocal elasticity and dispersion of plane waves", *International Journal of Engineering Science*, Vol. 10, No. 5, (1972), 425-435.
21. Eringen, A.C., "Nonlocal continuum field theories", Springer Science & Business Media, (2002).
22. Duan, W., Wang, C.M. and Zhang, Y., "Calibration of nonlocal scaling effect parameter for free vibration of carbon nanotubes by molecular dynamics", *Journal of Applied Physics*, Vol. 101, No. 2, (2007), 24305-24305.
23. Shen, L., Shen, H.-S. and Zhang, C.-L., "Nonlocal plate model for nonlinear vibration of single layer graphene sheets in thermal environments", *Computational Materials Science*, Vol. 48, No. 3, (2010), 680-685.
24. Wang, Q. and Wang, C., "The constitutive relation and small scale parameter of nonlocal continuum mechanics for modelling carbon nanotubes", *Nanotechnology*, Vol. 18, No. 7, (2007).
25. Semmah, A., Tounsi, A., Zidour, M., Heireche, H. and Naceri, M., "Effect of the chirality on critical buckling temperature of zigzag single-walled carbon nanotubes using the nonlocal continuum theory", *Fullerenes, Nanotubes and Carbon Nanostructures*, Vol. 23, No. 6, (2015), 518-522.
26. Reddy, J., "Nonlocal theories for bending, buckling and vibration of beams", *International Journal of Engineering Science*, Vol. 45, No. 2, (2007), 288-307.
27. Wang, C., Xiang, Y., Yang, J. and Kitipornchai, S., "Buckling of nano-rings/arches based on nonlocal elasticity", *International Journal of Applied Mechanics*, Vol. 4, No. 03, (2012).

28. Murmu, T. and Pradhan, S., "Buckling of biaxially compressed orthotropic plates at small scales", *Mechanics Research Communications*, Vol. 36, No. 8, (2009), 933-938.
29. Aksencer, T. and Aydogdu, M., "Levy type solution method for vibration and buckling of nanoplates using nonlocal elasticity theory", *Physica E: Low-dimensional Systems and Nanostructures*, Vol. 43, No. 4, (2011), 954-959.
30. Murmu, T. and Pradhan, S., "Buckling analysis of a single-walled carbon nanotube embedded in an elastic medium based on nonlocal elasticity and timoshenko beam theory and using dqm", *Physica E: Low-dimensional Systems and Nanostructures*, Vol. 41, No. 7, (2009), 1232-1239.
31. Pradhan, S. and Murmu, T., "Small scale effect on the buckling analysis of single-layered graphene sheet embedded in an elastic medium based on nonlocal plate theory", *Physica E: Low-dimensional Systems and Nanostructures*, Vol. 42, No. 5, (2010), 1293-1301.
32. Sedighi, H.M., Keivani, M. and Abadyan, M., "Modified continuum model for stability analysis of asymmetric FGM double-sided nems: Corrections due to finite conductivity, surface energy and nonlocal effect", *Composites Part B: Engineering*, Vol. 83, (2015), 117-133.
33. Sedighi, H.M., "The influence of small scale on the pull-in behavior of nonlocal nanobridges considering surface effect, casimir and van der waals attractions", *International Journal of Applied Mechanics*, Vol. 6, No. 03, (2014).
34. Sedighi, H.M., Daneshmand, F. and Abadyan, M., "Modified model for instability analysis of symmetric fgm double-sided nano-bridge: Corrections due to surface layer, finite conductivity and size effect", *Composite Structures*, Vol. 132, (2015), 545-557.
35. Dastjerdi, S. and Jabbarzadeh, M., "A non-linear static equivalent model for multi-layer annular/circular graphene sheet based on non-local elasticity theory considering third order shear deformation theory in thermal environment", *International Journal of Engineering Science*, Vol. 28, No. 10, (2015), 1533-1542.
36. Naderi, A. and Baradaran, G., "Element free galerkin method for static analysis of thin micro/nanoscale plates based on the nonlocal plate theory", *International Journal of Engineering*, Vol. 26, (2013), 795-806.
37. Amiri, A., Fakhari, S., Pournaki, I., Rezazadeh, G. and Shabani, R., "Vibration analysis of circular magneto-electro-elastic nanoplates based on eringen's nonlocal theory", *International Journal of Engineering-Transactions C: Aspects*, Vol. 28, No. 12, (2015), 1808-1817.
38. Duan, W. and Wang, C.M., "Exact solutions for axisymmetric bending of micro/nanoscale circular plates based on nonlocal plate theory", *Nanotechnology*, Vol. 18, No. 38, (2007).
39. Farajpour, A., Mohammadi, M., Shahidi, A. and Mahzoon, M., "Axisymmetric buckling of the circular graphene sheets with the nonlocal continuum plate model", *Physica E: Low-Dimensional Systems and Nanostructures*, Vol. 43, No. 10, (2011), 1820-1825.
40. Babaei, H. and Shahidi, A.R., "Small-scale effects on the buckling of quadrilateral nanoplates based on nonlocal elasticity theory using the galerkin method", *Archive of Applied Mechanics*, Vol. 81, (2011), 1051-1062.
41. Malekzadeh, P., Setoodeh, A. and Beni, A.A., "Small scale effect on the thermal buckling of orthotropic arbitrary straight-sided quadrilateral nanoplates embedded in an elastic medium", *Composite Structures*, Vol. 93, No. 8, (2011), 2083-2089.
42. Anjomshoa, A., "Application of Ritz functions in buckling analysis of embedded orthotropic circular and elliptical micro/nano-plates based on nonlocal elasticity theory", *Meccanica*, Vol. 48, No. 6, (2013), 1337-1353.
43. Ravari, M.K. and Shahidi, A., "Axisymmetric buckling of the circular annular nanoplates using finite difference method", *Meccanica*, Vol. 48, No. 1, (2013), 135-144.
44. Sun, Y. and Xia, Y., "Triangular nanoplates of silver: Synthesis, characterization, and use as sacrificial templates for generating triangular nanorings of gold", *Advanced Materials*, Vol. 15, No. 9, (2003), 695-699.
45. Sun, Y., Mayers, B. and Xia, Y., "Transformation of silver nanospheres into nanobelts and triangular nanoplates through a thermal process", *Nano Letters*, Vol. 3, No. 5, (2003), 675-679.
46. Tham, L. and Szeto, H., "Buckling analysis of arbitrarily shaped plates by spline finite strip method", *Computers & Structures*, Vol. 36, No. 4, (1990), 729-735.
47. Karami, G., Shahpari, S.A. and Malekzadeh, P., "Dqm analysis of skewed and trapezoidal laminated plates", *Composite Structures*, Vol. 59, No. 3, (2003), 393-402.
48. Fletcher, C.A., "Computational galerkin methods", Springer, (1984).
49. Leung, A. and Mao, S., "A symplectic galerkin method for non-linear vibration of beams and plates", *Journal of Sound and Vibration*, Vol. 183, No. 3, (1995), 475-491.
50. Long, S. and Atluri, S., "A meshless local petrov-galerkin method for solving the bending problem of a thin plate", *Computer Modeling in Engineering and Sciences*, Vol. 3, No. 1, (2002), 53-64.
51. Dowell, E., "Nonlinear flutter of curved plates", *AIAA Journal*, Vol. 7, No. 3, (1969), 424-431.
52. Chen, X., Liu, G. and Lim, S., "An element free galerkin method for the free vibration analysis of composite laminates of complicated shape", *Composite Structures*, Vol. 59, No. 2, (2003), 279-289.
53. Kerr, A.D., "Elastic and viscoelastic foundation models", *Journal of Applied Mechanics*, Vol. 31, No. 3, (1964), 491-498.
54. Wang, C. and Liew, K., "Buckling of triangular plates under uniform compression", *Engineering Structures*, Vol. 16, No. 1, (1994), 43-50.

**APPENDIX**

$$\begin{aligned}
 \Pi(x, y) = & D_{11}W_{,xx}\chi_{,xx} + D_{12}\left[W_{,xx}\chi_{,yy} + W_{,yy}\chi_{,xx}\right] + D_{22}W_{,yy}\chi_{,yy} + 4D_{33}W_{,xy}\chi_{,xy} \\
 & + k_w\left[W\chi + \mu\left(W_{,x}\chi_{,x} + W_{,y}\chi_{,y}\right)\right] + k_p\left[W_{,x}\chi_{,x} + W_{,y}\chi_{,y} + \mu\left(W_{,xx}\chi_{,xx} + 2W_{,xy}\chi_{,xy} + W_{,yy}\chi_{,yy}\right)\right] \\
 & - \omega^2\left\{m_0\left[W\chi + \mu\left(W_{,x}\chi_{,x} + W_{,y}\chi_{,y}\right)\right] + m_2\left[W_{,x}\chi_{,x} + W_{,y}\chi_{,y} + \mu\left(W_{,xx}\chi_{,xx} + 2W_{,xy}\chi_{,xy} + W_{,yy}\chi_{,yy}\right)\right]\right\} \\
 & + N_{xx}\left[W_{,x}\chi_{,x} + \mu\left(W_{,xx}\chi_{,xx} + W_{,yy}\chi_{,yy}\right)\right] + N_{yy}\left[W_{,y}\chi_{,y} + \mu\left(W_{,xy}\chi_{,xy} + W_{,yy}\chi_{,yy}\right)\right] \\
 & + N_{xy}\left[W_{,x}\chi_{,y} + W_{,y}\chi_{,x} + \mu\left(W_{,xx}\chi_{,xy} + W_{,xy}\chi_{,xx} + W_{,yy}\chi_{,xy} + W_{,xy}\chi_{,yy}\right)\right]
 \end{aligned} \tag{A.1}$$

$$\begin{aligned}
 \Lambda(s) = & \chi\left\{W_{,xxx}\left(D_{11} + \mu(k_p - m_2\omega^2 + N_{xx})\right)n_x + W_{,xyy}\left(D_{12} + \mu(k_p - m_2\omega^2 + N_{yy} + 2N_{xy}\frac{n_x}{n_y})\right)n_y + W_{,yyy}\left(D_{12}\right. \right. \\
 & \left. \left. + 4D_{33} + \mu(k_p - m_2\omega^2 + N_{xx} + 2N_{xy}\frac{n_y}{n_x})\right)n_x + W_{,yyy}\left(D_{22} + \mu(k_p - m_2\omega^2 + N_{yy})\right)n_y - W_{,x}\left(k_p - m_2\omega^2 + N_{xx}\right. \right. \\
 & \left. \left. + N_{xy}\frac{n_y}{n_x} + \mu(k_w + m_0\omega^2)\right)n_x - W_{,y}\left(k_p - m_2\omega^2 + N_{xy}\frac{n_x}{n_y} + N_{yy} + \mu(k_w + m_0\omega^2)\right)n_y\right\}
 \end{aligned} \tag{A.2}$$

$$\begin{aligned}
 & - \chi_{,x}\left\{W_{,xx}\left(D_{11} + \mu(k_p - m_2\omega^2 + N_{xx} + N_{xy}\frac{n_y}{n_x})\right)n_x + W_{,xy}\left(4D_{33} + \mu(k_p - m_2\omega^2 + N_{xx} + N_{xy}\frac{n_x}{n_y})\right)n_y \right. \\
 & \left. W_{,yy}\left(D_{12}n_x\right)\right\} - \chi_{,y}\left\{W_{,yy}\left(D_{22} + \mu(k_p - m_2\omega^2 + N_{xy}\frac{n_x}{n_y} + N_{yy})\right)n_y + \mu W_{,xy}\left(k_p - m_2\omega^2 + N_{xy}\frac{n_y}{n_x}\right. \right. \\
 & \left. \left. + N_{yy}\right)n_x + W_{,xx}\left(D_{12}n_y\right)\right\} \\
 K_{ij} = & \iint_R \left[ D_{11} \frac{\partial^2 \Phi_i}{\partial x^2} \frac{\partial^2 \Phi_j}{\partial x^2} + D_{12} \left( \frac{\partial^2 \Phi_i}{\partial x^2} \frac{\partial^2 \Phi_j}{\partial y^2} + \frac{\partial^2 \Phi_i}{\partial y^2} \frac{\partial^2 \Phi_j}{\partial x^2} \right) + D_{22} \frac{\partial^2 \Phi_i}{\partial y^2} \frac{\partial^2 \Phi_j}{\partial y^2} + 4D_{33} \frac{\partial^2 \Phi_i}{\partial x \partial y} \frac{\partial^2 \Phi_j}{\partial x \partial y} \right] dx dy
 \end{aligned} \tag{A.3}$$

$$\begin{aligned}
 M_{ij} = & \iint_R \left\{ m_0 \left[ \Phi_i \Phi_j + \mu \left( \frac{\partial \Phi_i}{\partial x} \frac{\partial \Phi_j}{\partial x} + \frac{\partial \Phi_i}{\partial y} \frac{\partial \Phi_j}{\partial y} \right) \right] \right. \\
 & \left. + m_2 \left( \frac{\partial \Phi_i}{\partial x} \frac{\partial \Phi_j}{\partial x} + \frac{\partial \Phi_i}{\partial y} \frac{\partial \Phi_j}{\partial y} + \mu \left( \frac{\partial^2 \Phi_i}{\partial x^2} \frac{\partial^2 \Phi_j}{\partial x^2} + 2 \frac{\partial^2 \Phi_i}{\partial x \partial y} \frac{\partial^2 \Phi_j}{\partial x \partial y} + \frac{\partial^2 \Phi_i}{\partial y^2} \frac{\partial^2 \Phi_j}{\partial y^2} \right) \right) \right\} dx dy
 \end{aligned} \tag{A.4}$$

$$\begin{aligned}
 B_{ij} = & \iint_R \left\{ \frac{\partial \Phi_i}{\partial x} \frac{\partial \Phi_j}{\partial x} + \mu \left( \frac{\partial^2 \Phi_i}{\partial x^2} \frac{\partial^2 \Phi_j}{\partial x^2} + \frac{\partial^2 \Phi_i}{\partial x \partial y} \frac{\partial^2 \Phi_j}{\partial x \partial y} \right) + \frac{N_{yy}}{N_{xx}} \left[ \frac{\partial \Phi_i}{\partial y} \frac{\partial \Phi_j}{\partial y} + \mu \left( \frac{\partial^2 \Phi_i}{\partial y^2} \frac{\partial^2 \Phi_j}{\partial y^2} + \frac{\partial^2 \Phi_i}{\partial x \partial y} \frac{\partial^2 \Phi_j}{\partial x \partial y} \right) \right] \right. \\
 & \left. + \frac{N_{xy}}{N_{xx}} \left[ \left( \frac{\partial \Phi_i}{\partial x} \frac{\partial \Phi_j}{\partial y} + \frac{\partial \Phi_i}{\partial y} \frac{\partial \Phi_j}{\partial x} \right) + \mu \left( \frac{\partial^2 \Phi_i}{\partial x^2} \frac{\partial^2 \Phi_j}{\partial x \partial y} + \frac{\partial^2 \Phi_i}{\partial x \partial y} \frac{\partial^2 \Phi_j}{\partial x^2} + \frac{\partial^2 \Phi_i}{\partial y^2} \frac{\partial^2 \Phi_j}{\partial x \partial y} + \frac{\partial^2 \Phi_i}{\partial x \partial y} \frac{\partial^2 \Phi_j}{\partial y^2} \right) \right] \right\} dx dy
 \end{aligned} \tag{A.5}$$

## Nonlocal Effect on Buckling of Triangular Nano-composite Plates

A. R. Shahidi <sup>a</sup>, A. Anjomshoa <sup>a</sup>, S. H. Shahidi <sup>a</sup>, E. Raeisi Estabragh <sup>b</sup>

<sup>a</sup> Department of Mechanical Engineering, Isfahan University of Technology, Isfahan, Iran

<sup>b</sup> Department of Mechanical Engineering, University of Jiroft, Jiroft, Iran

### PAPER INFO

### چکیده

#### Paper history:

Received 08 December 2015

Received in revised form 12 January 2016

Accepted 03 March 2016

#### Keywords:

Buckling Analysis

Small Scale Effect

Nonlocal Elasticity Theory

Triangular Nano-composite Plate

Galerkin Method

در مطالعه حاضر اثرات مقیاس کوچک بر بارهای بحرانی کمانشی نانوصفحات کامپوزیتی مثلثی تحت بارگذاری فشاری یکنواخت درون صفحه‌ای بررسی شده‌است. از آنجا که در مقیاس کوچک ساختار صفحات گسسته است و اثر نیروهای چسبیده طویل برد قابل ملاحظه می‌شود، تئوری الاستیسته مقیاس‌پذیر غیرمحلی برای بسط دادن یک مدل پیوسته معادل برای نانوصفحات با در نظر گرفتن تغییر در رفتار مکانیکی آن‌ها بکار گرفته شده‌است. برای مدل‌سازی دقیق رفتار الاستیک ماتریس حول نانوصفحه از مدل الاستیک دو پارامتری وینکلر-پاسترناک استفاده شده‌است. در ادامه معادلات حاکم بر پایداری با استفاده از تئوری کلاسیک صفحات و اصل کار مجازی برای نانوصفحه کامپوزیتی مثلثی بدون نقص هندسی استخراج گردیده‌است. سپس از روش عددی معروف گالرکین به همراهی دستگاه مختصات مساحتی به عنوان مبنای روش حل استفاده شده‌است. روش حل حاضر کل نانوصفحه کامپوزیتی را به عنوان یک ابرالمان صفحه‌ای پیوسته با شکل دلخواه در نظر می‌گیرد. اثر پارامتر غیر محلی، ابعاد، نسبت منظر، مودهای کمانشی، ناهمسانگردی، تکیه‌گاه‌ها در لبه و ماتریس الاستیک بر بارهای بحرانی مورد بررسی قرار گرفته‌است. نتایج نشان می‌دهد که تمامی این پارامترها تأثیر چشمگیری بر مشخصه‌های پایداری نانوصفحات کامپوزیتی دارند. نتایج بارهای بحرانی به‌طور مشهود به مقدار پارامتر غیرمحلی نانوصفحه کمانش یافته خصوصاً در ابعاد کوچک‌تر، نسبت منظر کمتر، مودهای کمانشی بالاتر، ناهمسانگردی بیشتر و تکیه‌گاه‌های محکم‌تر بستگی دارد. همچنین دیده شده پارامترهای ماتریس الاستیک، خصوصاً پارامتر وینکلر، تأثیر بسزایی بر اثر مقیاس کوچک دارند و می‌توانند منجر به کاهش یا افزایش آن شوند. استفاده از تئوری الاستیسته کلاسیک، به‌واسطه تخمین مقادیر زیاد برای بارهای بحرانی، می‌تواند به طراحی و تحلیل ناقص این نانو ساختارهای پر کاربرد منجر شود. نتایج حاصل از تحقیق حاضر می‌تواند در طراحی، تحلیل و بهینه‌سازی بسیاری از نانو سیستم‌ها نظیر نانو سیستم‌های الکترونیکی - مکانیکی که از نانوصفحات کامپوزیتی به عنوان اجزاء باربر بهره می‌گیرند مورد استفاده قرار گیرند. اگر چه دیده شده که پرکننده‌های نانو در نانوکامپوزیت‌ها با افزایش سختی خمشی استحکام کلی نانوصفحات کامپوزیتی را افزایش می‌دهند اما در مطالعه حاضر از سوی دیگر نشان داده شده که اثر مقیاس کوچک در نانو ساختارها، نانوصفحات در این پژوهش، استحکام نانوصفحات کامپوزیتی و در نتیجه بارهای بحرانی کمانشی آن را کاهش می‌دهد. در نتیجه اثر مقیاس کوچک نقش مهمی در طراحی و تحلیل این نانو ساختارها بازی می‌کند که باید به‌منظور جلوگیری از فروپاشی این ساختارها به‌طور دقیق و کامل مورد بررسی و توجه قرار گیرد. علاوه بر این روش حل مورد استفاده در مطالعه حاضر یک روش تعمیم‌یافته است که می‌تواند برای تحلیل نانوصفحات کامپوزیتی با شکل دلخواه مورد استفاده قرار گیرد که یک مزیت در مطالعه بهینه‌سازی ساختاری به‌شمار می‌رود.

doi: 10.5829/idosi.ije.2016.29.03c.16